Visualization of Hydrogen Atomic Orbitals Classification according to the Node Type

Sumio Tokita

Saitama University (Emeritus), 255 Shimo-Ohkubo, Sakura-ku, Saitama-shi, Saitama 338-8570, Japan
E-mail address: tokita@apc.saitama-u.ac.jp

(Received May 3, 2017; Accepted June 14, 2017)

A three dimensional representation of the probability density distribution of a hydrogen atomic orbital in a glass block was developed. The density of the dots sculptured in the glass block shows the probability density of finding an electron, so the nodal plane is well described as spherical shell(s), planar or conical node(s) where the dots cannot be found. Node types and their numbers are summarized in Table 2. Classification according to the node type leads to an observation of systematic regularity in hydrogen atomic orbitals. Relationship between a square of a complex atomic orbital and a real atomic orbital is explained. Advantage of the probability density sculpture in a spherical glass block is also discussed.

Key words: Electron Cloud, 3-dimensional Representation, Spherical Node, Planar Node Including z axis, Planar and Conical Node Symmetrical about z axis, Complex Atomic Orbital, Real Atomic Orbital, Probability Density Distribution

1. Prologue

J. J. Thomson discovered the electron in 1897 [1]. E. Rutherford discovered the atomic nucleus in 1911. These epoch-making findings in the history of science led to an atomic orbit model as a planet around the sun (Fig. 1).

This orbit model had a problem that the line spectrum emitted from excited hydrogen atoms could not be explained. N. Bohr solved the problem assuming that the energies of the electron in a hydrogen atom are quantized, but the atomic orbit model was incorrect because it was based on classical mechanics [2]. In 1924, L. de Broglie proposed that all moving particles such as electrons exhibit wave behavior. E. Schrödinger's equation, published in 1926, describes an electron as a wavefunction [3]. Such a wavefunction, describing a single electron, is called an "orbital" [4]. Although this concept was mathematically convenient, it was difficult to visualize. M. Born proposed that Schrödinger's wavefunction could be used to calculate the probability of finding an electron at any given location around the nucleus [5].

A novel method of visualization to record Born's probability densities in a glass block was developed by the use of a three-dimensional laser technique [6]. This model represents that the electron may exhibit the properties of both a wave and a particle [7, 8]. Conventional visualization methods cannot simultaneously show all the characteristic features of an atomic orbital, whereas a real image in a glass block in the present study allows us to recognize both the shape of the orbital and its wave character, such as the existence of spherical, planar and/or conical nodes, at the same time (Fig. 2).

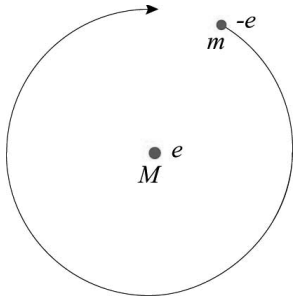

Fig. 1. An orbit model of a hydrogen atom.

In this paper, classification of hydrogen atomic orbitals with their node type was studied using this novel method of visualization.

2. Complex Hydrogen Atomic Orbitals

The Schrödinger equation (Eq. (1) in Fig. 1) describing the behavior of an electron in a hydrogen atom takes the form,

$$\left[-\frac{h^2}{8\pi^2 m}\left(\frac{\partial^2}{\partial x^2}+\frac{\partial^2}{\partial y^2}+\frac{\partial^2}{\partial z^2}\right)-k_0\frac{e^2}{r}\right]\chi = E\chi \quad (1)$$

where h, m, e, r and k_0 are Planck's constant, the mass of an electron, the elementary charge, the distance of the electron from the nucleus and an inverse of the dielectric constant under a vacuum (permittivity of free space). The atomic nucleus lies on the origin, and x, y, z are the coordinates of the electron. A procedure for solving the Schrödinger equation (Eq. (1)) to get orbital energies E and hydrogen atomic orbitals χ including complex counterparts Eq. (3) or real orbitals Eq. (4) is shown in Fig. 3 [9].

doi:10.5047/forma.2017.sii002

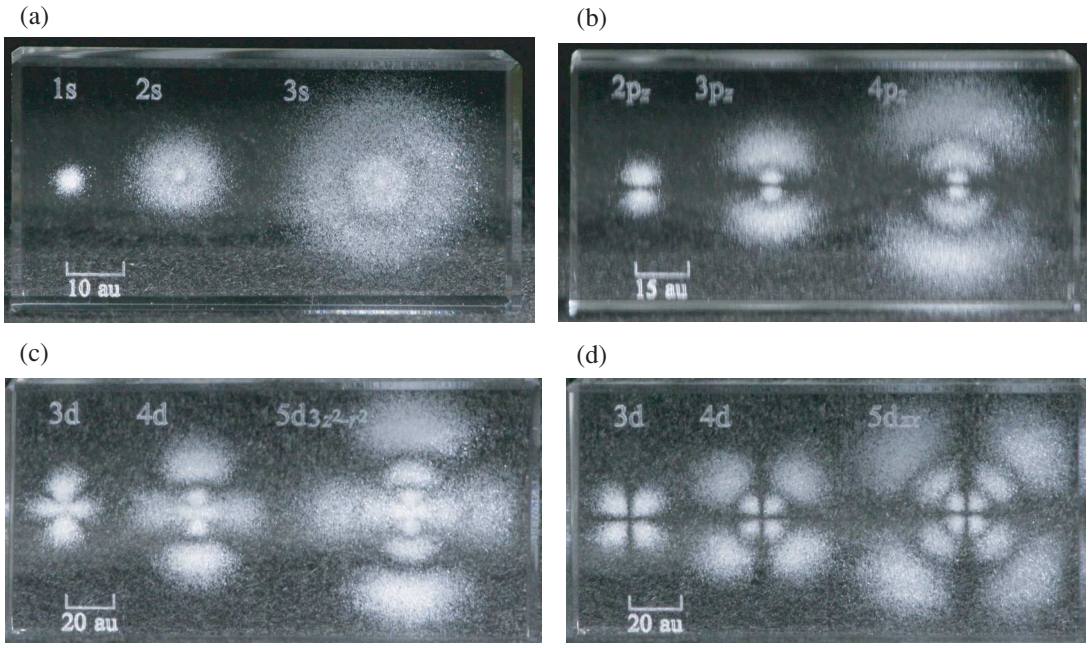

Fig. 2. Several examples of a novel visualization method to record Born's probability densities in a glass block by the use of a three-dimensional laser technique: (a): hydrogen 1s, 2s, and 3s orbitals; (b): 2p (z), 3p (z), and 4p (z) orbitals; (c): 3d ($3z^2 - r^2$), 4d ($3z^2 - r^2$), 5d ($3z^2 - r^2$) orbitals; (d): 3d (zx), 4d (zx), 5d (zx) orbitals. Glass size: $4 \times 4 \times 8$ cm.

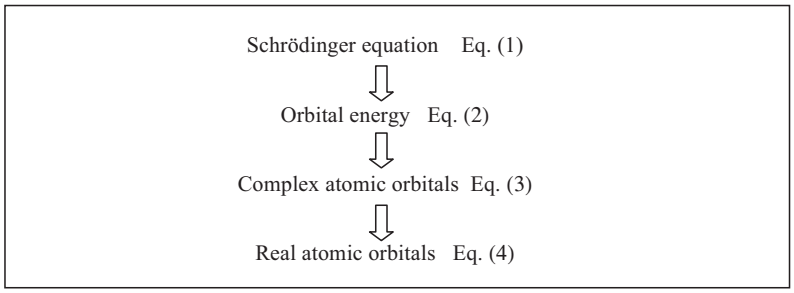

Fig. 3. An outline for solving the Schrödinger equation (Eq. (1)) to get hydrogen atomic orbitals Eq. (3) or (4).

Expanding the Cartesian coordinates (x, y, z) in the Schrödinger equation (Eq. (1)) into the spherical polar coordinates (r, θ, φ) (Fig. 4), the equation can be separated into functions of each coordinate to give orbital energies E_n (Eq. (2)) and atomic orbitals Eq. (3).

$$E_n = -\frac{13.60}{n^2}\text{eV} \tag{2}$$

$$\chi_{n,l,m} = R_{nl}(r)\Theta_{lm}(\theta)\Phi_m(\varphi). \tag{3}$$

$R_{nl}(r)$ are called radial distribution functions and $\Theta_{lm}(\theta)\Phi_m(\varphi)$ are called spherical harmonics. The well known real atomic orbitals Eq. (4) are obtained by the method mentioned in the following section.

$$\chi(x, y, z) \tag{4}$$

$$r = \sqrt{x^2 + y^2 + z^2} \tag{5}$$

$$z = r\cos\theta \tag{6}$$

$$\overline{\text{OQ}} = r\sin\theta \tag{7}$$

$$y = r\sin\theta\sin\varphi \tag{8}$$

$$x = r\sin\theta\cos\varphi. \tag{9}$$

Subscripts n, l, and m are the principal, azimuthal, and magnetic quantum number respectively, which take the following values.

$$n = 1, 2, 3, \ldots \tag{10}$$

$$l = 0, 1, 2, \ldots, n-1 \tag{11}$$

$$m = -l, -l+1, \ldots, 0, \ldots, l-1, l. \tag{12}$$

Orbitals with azimuthal quantum number $l = 0, 1, 2, 3, 4$ are designated s, p, d, f, g respectively. The letters then run alphabetically. The value of principal quantum number n is written in front of this letter. Table 1 summarizes the possible values of the quantum numbers l and m for values of n through $n = 4$.

Spherical harmonics $\Theta_{lm}(\theta)\Phi_m(\varphi)$ are functions that all contain $\exp(im\varphi)$ where $i = \sqrt{-1}$. In the case of $m \neq 0$, these functions are all complex.

3. Real Hydrogen Atomic Orbitals

By taking linear combinations of these complex (exponential) wavefunctions, the well known real atomic orbitals Eq. (4) are obtained [10–12]. Two examples of five 3d or-

Table 1. Designation and number of atomic orbitals based on quantum number n, l, and m.

Designation	n	l	m	Number	Total
1s	1	0	0	1	1
2s	2	0	0	1	4
2p		1	-1 0 1	3	
3s	3	0	0	1	9
3p		1	-1 0 1	3	
3d		2	-2 -1 0 1 2	5	
4s	4	0	0	1	16
4p		1	-1 0 1	3	
4d		2	-2 -1 0 1 2	5	
4f		3	-3 -2 -1 0 1 2 3	7	

Table 2. Nodes in hydrogen atomic orbitals.

Node type	Number of nodes
(A) Spherical nodes	$n-l-1$
(B) Planar and conical nodes symmetrical about z axis	$l-\|m\|$
(C) Planar nodes containing z axis	$\|m\|$
Total	$n-1$

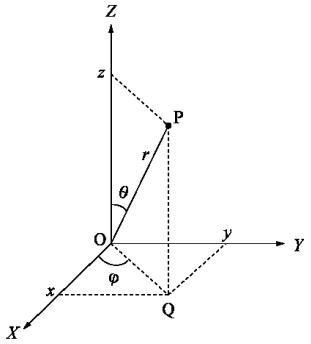

Fig. 4. Cartesian coordinates (x, y, z) and spherical polar coordinates (r, θ, φ).

bitals are shown below.

$$
\begin{aligned}
&-\frac{1}{\sqrt{2}}(\chi_{321}-\chi_{32-1})\\
&=\frac{1}{81\sqrt{2\pi}}\\
&\quad\cdot\exp(-r/3)zr\sin\theta\{-(-\exp(i\varphi)-\exp(-i\varphi))\}\\
&=\frac{2}{81\sqrt{2\pi}}\exp(-r/3)zx \qquad (13)
\end{aligned}
$$

$$
\begin{aligned}
&-\frac{1}{i\sqrt{2}}(\chi_{321}+\chi_{32-1})\\
&=\frac{1}{81i\sqrt{2\pi}}\\
&\quad\cdot\exp(-r/3)zr\sin\theta\{-(-\exp(i\varphi)+\exp(-i\varphi))\}\\
&=\frac{2}{81\sqrt{2\pi}}\exp(-r/3)yz. \qquad (14)
\end{aligned}
$$

Using equations Eqs. (6), (8), and (9) in Fig. 4, the spherical polar coordinates (r, θ, φ) in Eq. (13) or (14) are transformed into the Cartesian coordinates (x, y, z) [12, equations (S13), (S14)]. Using the Cartesian coordinates thus obtained, these orbitals are called 3d (zx) or 3d (yz). Orbital designations in the caption of Fig. 2 have the same meaning. As is shown below, the polynomials in the parentheses are important for the decision of the equation(s) of nodal plane(s).

4. Types of Nodes in Hydrogen Atomic Orbitals

In the diagram of probability density distribution model, we can compare the size of the orbitals from their distribution regions (Fig. 2). The density of the dots sculptured in the glass block shows the probability density of finding an electron, so the nodal plane is well described as spherical shell(s) or planar and conical node(s) symmetrical about z axis where the dots cannot be found. Number of these nodes together with planar nodes including z axis in hydrogen atomic orbitals is summarized in Table 2 in terms of n, l, and m [13].

There are three types of nodes in hydrogen atomic orbitals.

[A] Spherical nodes: In Fig. 2(a), (b), (c), or (d), we can observe 0 (left), 1 (center), or 2 (right) dark circle(s) respectively. These circles correspond to spherical nodes.

[B] Planar and conical nodes symmetrical about z axis (lateral surfaces of right circular cones): In Fig. 2(c), V or Λ (reversely V) shaped dark area is observed at left, center, and right pictures respectively. These are lateral surfaces of two cones (Fig. 5(b)). In Fig. 2(b), or 2(d), a dark horizontal line is observed. This can be considered to an utmost limit that the height (distance from an apex to a base) of a cone approaches to 0 to give a planar node (Fig. 5(a)).

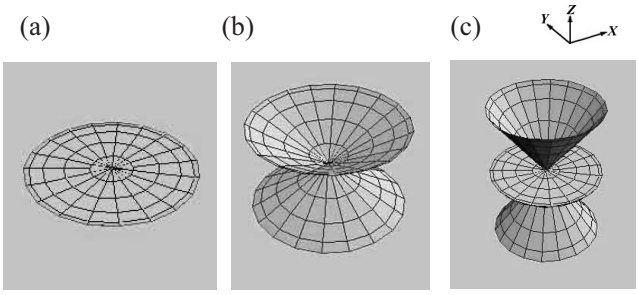

Fig. 5. Nodes in Figs. 2(b), (c) and 6.

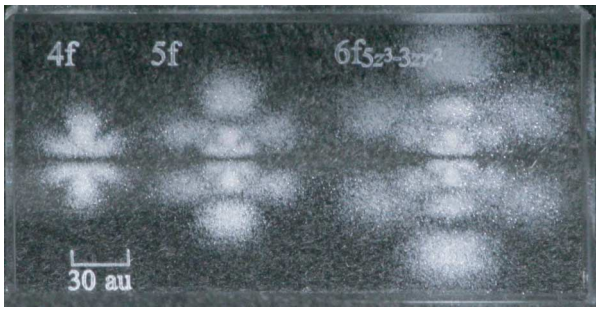

Fig. 6. 4f $(5z^3 - 3zr^2)$, 5f $(5z^3 - 3zr^2)$, 6f $(5z^3 - 3zr^2)$.

[C] Planar nodes containing z axis: In Fig. 2(d) a dark vertical line is observed. This planar node does not exist in the complex (exponential) wavefunction (Eq. (2)). By taking linear combinations of the exponential wavefunctions having the same n, l, and $|m|$ values, the real atomic orbitals Eq. (4) having $|m|$ planar nodes containing z axis are obtained.

5. Spherical Nodes (Category [A])

In the atomic orbitals $\chi_{n,l,m} = R_{nl}(r)\Theta_{lm}(\theta)\Phi_m(\varphi)$ Eq. (3), radial distribution function $R_{nl}(r)$ consists of polynomials of radial vector r. Using a software called "Mathematica (Wolfram Mathematica)" [14], these functions are conveniently given [15]. Radii of spherical nodes can be obtained by setting the value of these functions to 0. In the case of s orbitals, each spherical harmonics $\Theta_{lm}(\theta)\Phi_m(\varphi)$ has a constant value of $1/2\sqrt{\pi}$. They are therefore independent of θ and φ, and spherically symmetrical. 1 s orbital has no node ($n = 1$, $l = 0$, $n - l - 1 = 0$). Radii of spherical nodes in 2–7s orbitals are given below (1 au = 52.92 pm) [15]. A spherical node is also called a radial node.

1s: none
2s: 2 au
3s: 1.90192, 7.09808 au
4s: 1.87164, 6.61081, 15.5175 au
5s: 1.85823, 6.42909, 14.3279, 27.3847 au
6s: 1.85109, 6.3389, 13.8325, 25.1972, 42.7803 au
7s: 1.84684, 6.28705, 13.5682, 24.2159, 39.3211, 61.7609 au.

Radii of other spherical nodes, for example in Figs. 2(b), (c) and (d), are similarly obtained by the same method [14, 15].

6. Planar and Conical Nodes Symmetrical about z axis (Category [B])

Figures 2(b) and (c), or Fig. 6 shows orbitals having the same magnetic quantum number of $m = 0$. Figure 2(b) shows 2p (z), 3p (z), and 4p (z) orbitals. These orbitals have the same azimuthal quantum number of $l = 1$, the number of the node of category [B] is 1 ($l - |m| = 1 - 0 = 1$) as is shown in Fig. 5(a).

Figure 2(c) shows 3d $(3z^2 - r^2)$, 4d $(3z^2 - r^2)$, and 5d $(3z^2 - r^2)$ orbitals. These orbitals have the same azimuthal quantum number of $l = 2$, the number of the node of category [B] is 2($l - |m| = 2 - 0 = 2$) as is shown in Fig. 5(b).

Figure 6 shows 4f $(5z^3 - 3zr^2)$, 5f $(5z^3 - 3zr^2)$, and 6f $(5z^3 - 3zr^2)$ orbitals. These orbitals have the same azimuthal quantum number of $l = 3$, the number of the node of category [B] is 3 ($l - |m| = 3 - 0 = 3$) as is shown in Fig. 5(c).

Mathematical formulas of these nodes are obtained from the numerical expression in the parentheses of each orbital designation.

In the case of 2p (z), 3p (z), or 4p (z) orbital in Fig. 2(b), the numerical expression in the parentheses is z. Setting the value of this expression to 0, we obtain:

$$z = 0. \tag{15}$$

This formula represents XY plane in Fig. 5(a). Otherwise, using equation $z = r\cos\theta$ (Eq. (6)),

$$r\cos\theta = 0 \tag{16}$$

$$\therefore \theta = \pi/2. \tag{17}$$

Polar angle $\theta = 90^\circ$ also represents XY plane.

In the case of 3d $(3z^2 - r^2)$, 4d $(3z^2 - r^2)$, or 5d $(3z^2 - r^2)$ orbital in Fig. 2(c), the numerical expression in the parentheses is $3z^2 - r^2$. Setting the value of this expression to 0, we obtain:

$$3z^2 - r^2 = 0. \tag{18}$$

By the use of Eq. (6),

$$r^2(\sqrt{3}\cos\theta + 1)(\sqrt{3}\cos\theta - 1) = 0$$

$$\therefore \cos\theta = -1/\sqrt{3}, \cos\theta = 1/\sqrt{3} \tag{19}$$

namely,

$$\theta = 125.3^\circ, 54.74^\circ. \tag{20}$$

These formulas represent two cones in Fig. 5(b).

In the case of 4f $(5z^3 - 3zr^2)$, 5f $(5z^3 - 3zr^2)$, or 6f $(5z^3 - 3zr^2)$ orbital in Fig. 6, the numerical expression in the parentheses is $z(5z^2 - 3r^2)$. By the similar treatment as above, we obtain:

$$\theta = 90^\circ, 39.23^\circ, 140.8^\circ. \tag{21}$$

These formulas represent an XY plane and two cones in Fig. 5(c).

Similarly, by putting the polynomials of variables z and r to 0, mathematical formulas of the nodes of category [B] are obtained.

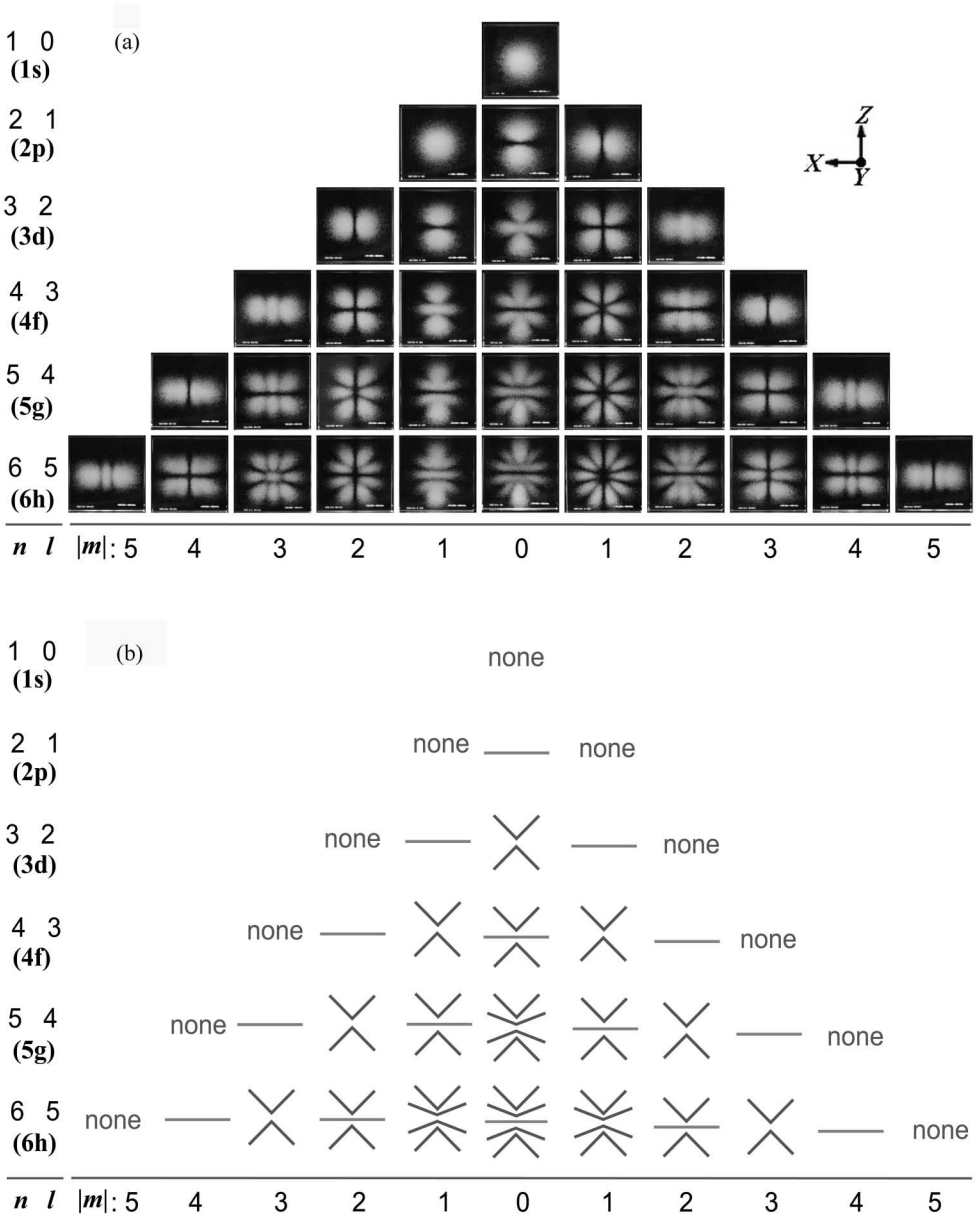

Fig. 7. (a) Probability density distribution in the 3-dimensional representation of the squares of hydrogen atomic orbitals observing through y axis. Glass size: $4 \times 4 \times 4$ cm. (b) Schematic representation of the planar and conical nodes symmetrical about z axis.

Figure 7(a) shows 36 orbitals for values of principal quantum number n from 1 to 6, and values of azimuthal quantum number $l = n - 1$. These orbitals have no spherical node. Looking through the y axis, we can observe planar and conical nodes symmetrical about z axis (category [B]). The patterns of these nodes are symbolically shown in Fig. 7(b) [16]. The orbital at the top of each column has no node of category [B] as is represented none in Fig. 7(b). The number of nodes of category [B] increases one by one as the value of n increases, and decreases one by one as the value of $|m|$ increases.

Total number of atomic orbitals for values of principal quantum number n from 1 to 6 is 91, as is calculated from Table 1 ($1+4+9+16+25+36 = 91$). In these, $55(91-36)$ orbitals have spherical node(s).

7. Planar Nodes Containing z axis (Category [C])

Figure 8(a) shows 36 sculptured cubes in Fig. 7(a) turned 180 degrees around z axis and 90 degrees around x axis. Looking through the z axis, we can observe planar nodes containing z axis (category [C]). The orbital at the top of Figs. 7(a) and 8(a) is a 1s orbital. As s orbitals have spherical symmetry, the shapes of these two pictures are identical. In the second rows, 2p (y), 2p (z), and 2p (x) orbitals are shown. Comparing Fig. 7(a) with Fig. 8(a), these three orbitals have the same shapes having different direction of nodal planes.

The number of planar nodes containing z axis (category [C]) is the absolute of magnetic quantum number $|m|$ (Table 2). For example, the value of magnetic quantum number m of 1s or 2p (z) orbital is 0, each orbital has no planar nodes containing z axis as is shown as none in Fig. 8(b).

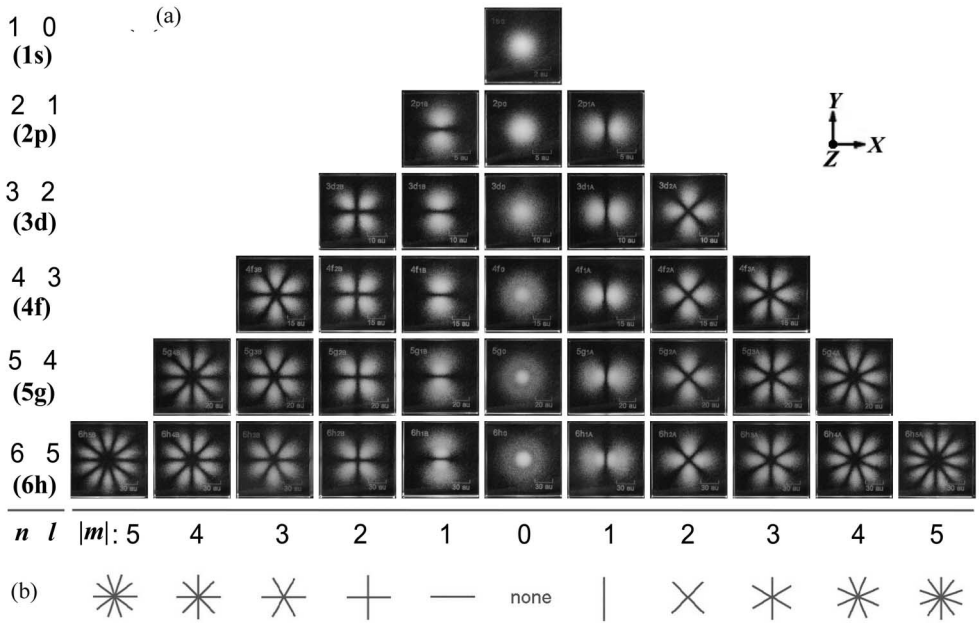

Fig. 8. (a) Probability density distribution in the 3-dimensional representation of the squares of hydrogen atomic orbitals observing through z axis Glass size: $4 \times 4 \times 4$ cm. (b) Schematic representation of the planar nodes containing z axis.

In the case of 2p (y) or 2p (x) orbital, $|m|$ is equal to 1, corresponding to a single horizontal or vertical line in Fig. 8(b) [16].

In Fig. 8(a), the absolute value of magnetic quantum number $|m|$ is the same in every orbital drawn up in a column, giving the same pattern as is shown in Fig. 8(b).

In the case of $m \neq 0$, there exists a pair of orbitals having the same quantum number n, l, and $|m|$. When rotating around z axis by 90 degrees/$|m|$, the planar nodes containing z axis in one part of this pairing orbitals can be transformed to the pattern of corresponding nodes of the other part of the pairing orbitals.

At a glance, the form of atomic orbitals seems to be full of chaos [17], however, by the classification according to the node type in Fig. 7(a) or Fig. 8(a), we can see systematic regularity shown in Fig. 7(b) or Fig. 8(b).

8. Relationship between an Absolute Square of Complex Atomic Orbital and a Real Atomic Orbital

In the case of $m \neq 0$, atomic orbital functions (3) in Fig. 3 are all complex. Isosurfaces of squares of these complex and also $m = 0$ wavefunctions are shown in Fig. 9(a). By taking linear combinations of a pair of complex wavefunctions, the well known real atomic orbitals (4) are obtained [10–12]. Isosurfaces of these real wavefunctions are shown in Fig. 9(b).

Examples to obtain "real function form" by slicing up "absolute square of complex function form" of hydrogen 3d orbitals with $|m|$ planar node(s) are shown in Fig. 10 [17–19].

When $n = 3$, $l = 2$, and $m = 0$ (Fig. 10(a)), there exists no planar node containing z axis. There is no slicing up, therefore, the shapes of the resultant orbital (bottom) are the same as the top view except for their mathematical signs expressed by their colors.

When $n = 3$, $l = 2$, and $|m| = 1$, the number of planar nodes containing z axis is 1. The mathematical process to give Eq. (13) can be viewed geometrically as slicing up the two doughnuts with one planar node containing z axis (Fig. 10(b) top, right) and with the edges rounded off to get the clover type 3d (xz) orbital (Fig. 10(b) bottom, right). As for the Eq. (14), slicing the two doughnuts with a node perpendicular to this (Fig. 10(b) top, left), we get the pairing clover type 3d (yz) orbital (Fig. 10(b) bottom, left).

When $n = 3$, $l = 2$, and $|m| = 2$, the number of planar nodes containing z axis is 2, therefore, two equally spaced planar nodes are used to slice a single doughnut, the familiar clover type four lobes of 3d ($x^2 - y^2$) orbital is given (Fig. 10(c), right). When the two equally spaced planar nodes are rotated around z axis for 45 degrees and are used to slice a single doughnut, the familiar clover type four lobes of 3d (xy) orbital is given (Fig. 10(c), left).

Figure 9(b) shows the result of slicing the "doughnut-like" lobes into lobes using $|m|$ planar nodes containing z axis. For each non-zero value of $|m|$, a pair of real orbitals are given. These two orbitals have the same shape and by the rotation around the z axis by 90 degrees/$|m|$, one of the pair is transformed into the other pair. In Fig. 9(b), only one of the pair is shown.

A three dimensional representation of the probability density of a complex or real hydrogen atomic orbital in a spherical glass block was developed. Different from a cubic media in Fig. 7(a) or 8(a), a spherical media has no edge. This advantage is effective for the observation of $n = 1, 2, \ldots, l = n - 1, m = 2$ orbitals. In the case of fourth column in Fig. 8(a), planar nodes containing z axis is clearly seen as is shown the one of them in the fourth column in Fig. 7(a). However, as for the pairing orbitals shown in the eighth column in Fig. 8(a), it is difficult to observe planar nodes containing z axis because of the hindrance of

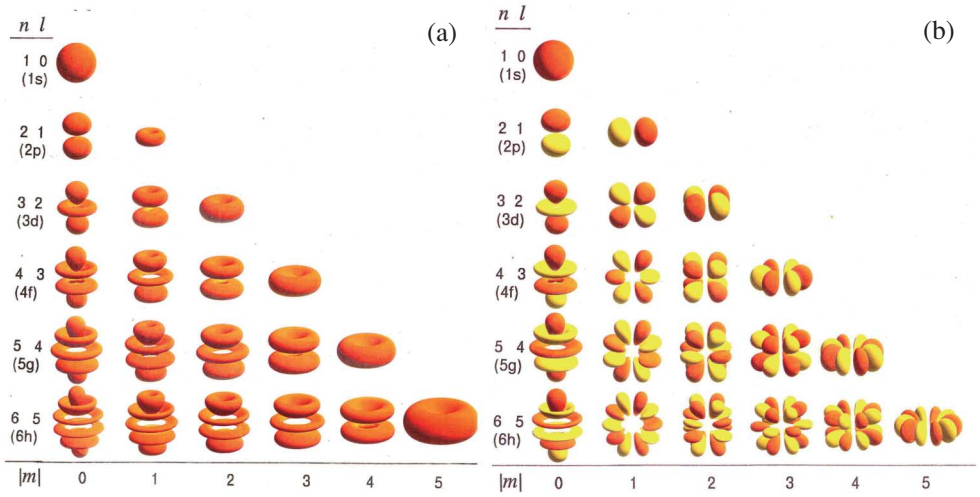

Fig. 9. Isosurfaces of (a) the absolute squares of hydrogen imaginary atomic orbitals and (b) real functionalized atomic orbitals.

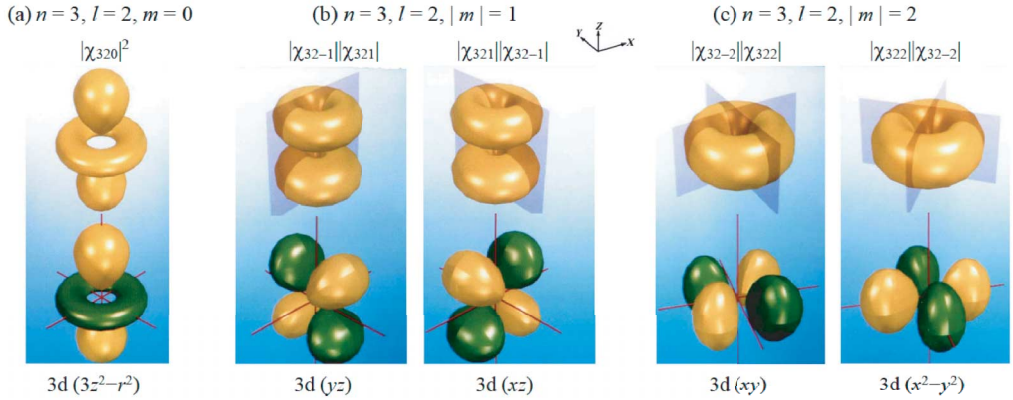

Fig. 10. Obtaining the "real function form" (bottom) by slicing up the "absolute square of complex function form" (top) with $|m|$ planar node(s) [17–19].

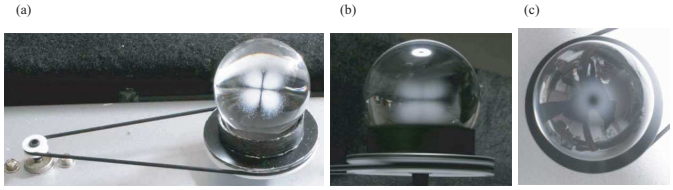

Fig. 11. (a) A 4f $(zx^2 - zy^2)$ (or 4f (xyz)) hydrogen atomic orbital model set on a plate for revolving. (b) Side view of the revolving image. (c) Top view of the revolving image.

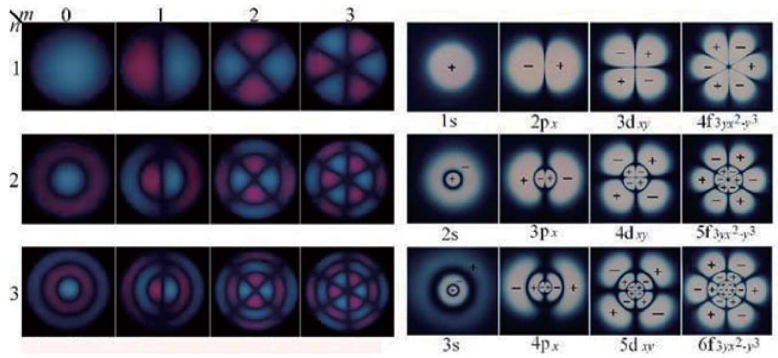

Fig. 12. (a) Characteristic pattern of standing waves of a 2-dimensional circular membrane of uniform thickness, attached to a rigid frame (n: number of radial nodes; m: number of azimuthal nodes). (b) Cross section on the x-y plane of 3-dimensional hydrogen atomic orbitals.

edges (the plane $x = y$, or $x = -y$ coalesces into edges parallel to the z axis). Another advantage of no edge effect lies on the total amount of the sculpture. As the one shape of the pairing orbitals transformed to the other by a proper rotation, 36 sculptures in Fig. 7(a) or 8(a) are diminished to 21 patterns listed in Fig. 9(b). The greatest advantage of this sculpture lies in the appearance of the image of an absolute square of complex orbital in Fig. 9(a) by revolving a spherical glass block of the probability density of a real hydrogen atomic orbital. Figure 11(a) shows a hydrogen 4f $(zx^2 - zy^2)$ (or 4f (xyz)) orbital, namely, an $n = 4$, $l = 3$, $m = 2$ orbital set on a plate for revolving. On revolving, the image of an $n = 4$, $l = 3$, $|m| = 2$ orbital of Fig. 9(a) appears (Figs. 11(b) and (c)) [20, 21].

9. Epilogue

3-D isosurface model (Figs. 9 and 10) hardly shows the entire region where an electron can be found. On the other hand, in the diagram of probability density distribution models in a glass block (Figs. 2, 6, 7(a), 8(a) and 11), an electron is found everywhere around the nucleus. In the diagram of probability density distribution model, we can compare the size of the orbitals from their distribution regions (Figs. 2 and 6). The density of the dots sculptured in the glass block shows the probability density of finding an electron, so the nodal plane is well described as spherical shell(s) (Figs. 2 and 6), planar or conical node(s) symmetrical about z axis (Fig. 7), or planar node(s) containing z axis (Fig. 8) where the dots cannot be found. Number of these nodes in hydrogen atomic orbitals is summarized in Table 2. The form of atomic orbitals seems to be full of chaos [17], however, by the classification according to the node type in Fig. 7(a) or Fig. 8(a) we can see systematic regularity shown in Fig. 7(b) or Fig. 8(b).

K. Miyazaki stated that the word "Science on Form" has fascinating and rather magical power because an analogy on form is observed over a wide area of scientific investigation [22]. Vibrations of a circular membrane of a kettledrum are known to be simulated by the use of Bessel functions [23, 24]. Figure 12(a) shows the result of these simulations to give the two-dimensional membrane moving in a characteristic pattern of standing waves. Topological analogy is observed in Fig. 12(b) representing a cross section of hydrogen atomic orbitals [25].

The above-mentioned studies on hydrogen atomic orbitals are now developed to the visualization of several molecular orbitals [26, 27], hybridized orbitals of organic molecules or metal complexes [28], sculpture of molecular form with electron clouds [29], and a study on n-dimensional atomic orbitals [30].

References

[1] S. Glastone, *The Structure of the Atom*, G. P. Thomson, *The Electron*, United States Energy Research and Development Administration (1972), Japanese ed., Shoji Ishida, *Genshi to Denshi no Sekai*, Tokai Univ. Press (1976).

[2] L. M. Brown, A. Paris and B. Pippard eds., *Twentieth Century Physics*, IOC Publ. Ltd. (Bristol) (1995), Japanese ed., *20 Seiki no Butsurigaku I*, Maruzen Co. Ltd. (Tokyo) (1999).

[3] E. Schrödinger, *Ann. Phys.*, **79**, 489–527 (1926).

[4] E. Cartmell and G. W. A. Fowles, *Valency and Molecular Structure*, 4th ed., Butterworths Sci. Pub., London (1977) p. 36.

[5] M. Born, *Z. Phys.*, **37**, 863–867 (1926).

[6] N. Tokita, S. Tokita and T. Nagao, *J. Comput. Chem. Jpn.*, **5**, 153–158 (2006). doi:http://doi.org/10.2477/jccj.5.153

[7] A. Tonomura, J. Endo, T. Matsuda, T. Kawasaki and H. Ezawa, *Am. J. Phys.*, **57**, 117 (1989).

[8] A. Tonomura, *Ryosi Rikigaku wo Miru—Densisen Horogurafi no Chosen*, Iwanami Kagaku Raiburari, Iwanami Shoten, Tokyo (1995) (in Japanese).

[9] S. Tokita, *J. Comput. Chem. Jpn.*, **15**, A16–A20 (2015). doi:http://doi.org/10.2477/jccj.2015-0018, *Densi wo Egaku* (3) (in Japanese).

[10] T. Azumi, *Gakubu Gakusei no Tameno Ryosi Kagaku Kogi Noto, Zenpen (Lecture Note on Quantum Chemistry, Part 1)* (in Japanese) *Molecular Science* Vol. 5 (2011) No. 1, Archives, PAC0005, p. 313 (Chapter 5, p. 25). https://www.jstage.jst.go.jp/browse/molsci/5/1/_contents

[11] E. U. Condon and G. H. Shortley, *The Theory of Atomic Spectra*, Cambridge University Press, London (1935, reprinted 1959), p. 52, Eq. (17).

[12] https://www.jstage.jst.go.jp/article/jccj/15/1/15_2016-0002/_article/supplement/-char/ja/, *Densi wo Egaku* (5), supplement (in Japanese).

[13] S. Tokita, *J. Comput. Chem. Jpn.*, **14**, A38–A41 (2015). doi:http://doi.org/10.2477/jccj.2015-0049, *Densi wo Egaku* (4) (in Japanese).

[14] http://www.wolfram.com/mathematica/ http://www.wolfram.com/mathematica/new-in-11/?src=google&416-JA

[15] https://www.jstage.jst.go.jp/article/jccj/14/2/14_2015-0018/_article/supplement/-char/ja/, *Densi wo Egaku* (3), supplement (in Japanese).

[16] S. Tokita, *J. Comput. Chem. Jpn.*, **15**, A47–A50 (2016). doi:http://doi.org/10.2477/jccj.2016-0051, *Densi wo Egaku* (7) (in Japanese).

[17] G. L. Breneman, Order out of Chaos: Shapes of Hydrogen Orbitals, *Jour. Chem. Educ.*, **65**, 31–33 (1988).

[18] S. Tokita, *J. Comput. Chem. Jpn.*, **15**, A7–A12 (2016). doi:http://doi.org/10.2477/jccj.2016-0002, *Densi wo Egaku* (5) (in Japanese).

[19] S. Tokita, *Gendai Kagaku*, No. 213, p. 50–55 (1988(12)) (in Japanese).

[20] N. Tokita, S. Hoshi, Y. Tateno, Y. Kunugi, K. Nakamura and S. Tokita, *Gensi Kido no Kyukei Garasu Chokoku (Atomic Orbitals in Spherical Glass Blocks)*, Society of Computer Chemistry, Japan, 2014 Shunki-Nenkai Koen Yokoshu, 1D01, Tokyo Institute of Technology (Ohokayama) (2014), p. 28–29 (in Japanese).

[21] S. Tokita, *J. Comput. Chem. Jpn.*, *Densi wo Egaku* (8) (in preparation).

[22] Y. Ogawa and K. Miyazaki, eds, *Katachi no Kagaku*, Asakura Publishing, Tokyo (1987) (in Japanese), p. 198.

[23] W. C. Elmore and M. A. Heald, *Physics of Waves*, Dover Publications, New York (1985), p. 59–65.

[24] M. Kawahashi, S. Toyooka, H. Kato and S. Tokita, *Me de Miru Rikigaku*, Kodansha Ltd. (1990), frontispiece.

[25] S. Tokita, *Gendai Kagaku*, No. 211, p. 57–61 (1988(10)) (in Japanese).

[26] S. Tokita and N. Tokita, *Bunsi Kido no Garasunai Chokoku-Sono2-Kyoyaku Nijyu Ketugo no Hyoji*, Society of Computer Chemistry, Japan, 2010 Shunki-Nenkai Koen Yokoshu, RX03, Tokyo Institute of Technology (Ohokayama) (2010) (in Japanese).

[27] N. Tokita and S. Tokita, *Bunsi Kido no Garasunai Chokoku-Sono3-Mizu nado no Kihonteki Bunsi no Hyoji*, Society of Computer Chemistry, Japan, 2012 Shuki-Nenkai Koen Yokoshu, 1D02, Yamagata Univ. (Yamagata) (2012), p. 27–29 (in Japanese).

[28] S. Tokita and N. Tokita, *Bunsi Kido no Garasunai Chokoku-Tohshi no Koka no Kensho-sono2-*, Society of Computer Chemistry, Japan, 2010 Shunki-Nenkai Koen Yokoshu, RX01, Nagaoka Kosen (Nagaoka) (2010) (in Japanese).

[29] The name NEBULA was given to these novel developed sculptures. These are found on NEBULA's homepage. http://winmostar.just-size.jp/nebula/index.html

[30] H. Hosoya, F. Kido and S. Tokita, *n-Dimensional Periodic Tables of the Elements*, D. H. Rouvray and R. B. King, eds., *The Mathematics of the Periodic Table*, Nova Science Pub. Inc., New York (2006), p. 59–74.